Electronic Supplementary Material (ESI) for Energy & Environmental Science.

Supplementary Information for

Thermodynamic Origin of Dendrite Growth in Metal Anode Batteries

A. Hagopian,[1,2] M.-L. Doublet,[1,2] J.-S. Filhol[1,2]**

[1]*ICGM, University of Montpellier, CNRS, ENSCM, Montpellier, France*

[2]*RS2E French network on Electrochemical Energy Storage, FR5439, Amiens, France*

Corresponding authors: Marie-Liesse Doublet (marie-liesse.doublet@umontpellier.fr) and Jean-Sébastien Filhol (jean-sebastien.filhol@umontpellier.fr)

S1. Computational details associated to energetics

A. Energy correction for the homogeneous background

In the grand canonical DFT methodological framework, the potential of the studied system is varied by charging the unit cell, i.e. adding or subtracting electrons to the initially neutral system. A homogeneous background of the exactly opposite charge is smeared through the entire unit cell and an energy correction is applied to compensate for it and obtain the corrected energy E_{corr}. Details of how to obtain the expression for final correction can be found in previous works.[1–3] Herein, we only give the final correction:

$$E_{corr} = E_{DFT}^{0} + \frac{d_0}{d}\left(E_{DFT}(N_e) - E_{DFT}^{0} + e_0\int_0^{N_e} E_a(N)dN\right)$$

where E_{corr} is the corrected DFT energy, E_{DFT}^{0} is the energy obtained from DFT at zero charge (i.e. neutral unit cell), $E_{DFT}(N_e)$ is the DFT energy calculated for a number N_e of added/subtracted electrons, d_0 is the vacuum thickness, d is the size of the entire unit cell in the *z*-direction, e_0 is the unit charge, and $E_a(N)$ is the potential averaged over the unit cell. As we are in the grand canonical framework, the relevant energy for further work and analysis, i.e. the free electrochemical energy *F(E),* is obtained from:

$$F(E) = E_{corr} - N_e FE$$

where E_{corr} is the corrected energy to compensate for the homogeneous background, F is the Faraday constant, and *E* is the calculated potential of the unit cell. The potential in the middle of vacuum is defined as the vacuum potential E^{vac}. Difference between the Fermi energy E^{F} and the vacuum potential allows obtaining the work function, corresponding to the potential E of the system. Li, Na and Mg potential reference scales can be obtained from $E_{Li} = E - 1.46$, $E_{Na} = E - 1.79$, and $E_{Mg} = E - 2.13$, respectively.

B. Calculation of the potential of zero-charge and surface capacitance

The potential of zero-charge E_{hkl}^{PZC} corresponds to the potential value for which the surface charge of a given (hkl)-surface is equal to zero. To compute this value, one single calculation of the neutral surface is needed. From this neutral surface calculation, $E_{hkl}^{PZC} = E_{hkl}^{vac} - E_{hkl}^{F}$ is determined by extracting the vacuum potential E_{hkl}^{vac} from the potential grid and the Fermi level E_{hkl}^{F}, as obtained in the DFT calculation output. The

capacitance C_{hkl}^{s} is computed from a (hkl)-electro-capillary curve as it corresponds to its second order derivative. It appears in the derivation of Lippmann equation: $C_{hkl}^{s} = -\left.\frac{\delta^2 \Upsilon_{hkl}}{\delta E^2}\right|_{T,p,\{\mu_i\}}$.

S2. Whisker growth simulation

A. Symmetry breaking of the Wulff shape

While a Wulff structure is {hkl}-dominated, a dendrite-like shape can be obtained thanks to a symmetry breaking of some selected (*hkl*)-surfaces belonging to the same {*hkl*}-class. Examples are given in the Fig.2 and are detailed here (these structures are modeled with VESTA).[4] When a b*cc*-particle is {100}-dominated, a symmetry breaking favoring (lowering surface tension to increase the surface area) 4/6 {100}-surfaces (for instance (001), (100), (00$\bar{1}$) and ($\bar{1}$00) surfaces) induces a [100]-growth direction with a square cross section. When the particle is {110}-dominated, a symmetry breaking favoring 6/12 {110}-surfaces (for instance (0$\bar{1}$1), (1$\bar{1}$0), (10$\bar{1}$), (01$\bar{1}$), ($\bar{1}$10) and ($\bar{1}$01) surfaces) induces a [111]-growth direction with a hexagonal cross section. When the particle is {111}-dominated, a symmetry breaking favoring 4/8 {111}-surfaces (for instance (1$\bar{1}$1), (11$\bar{1}$), ($\bar{1}$1$\bar{1}$) and ($\bar{1}\bar{1}$1) surfaces) induces a [110]-growth direction with a rhombus cross section.

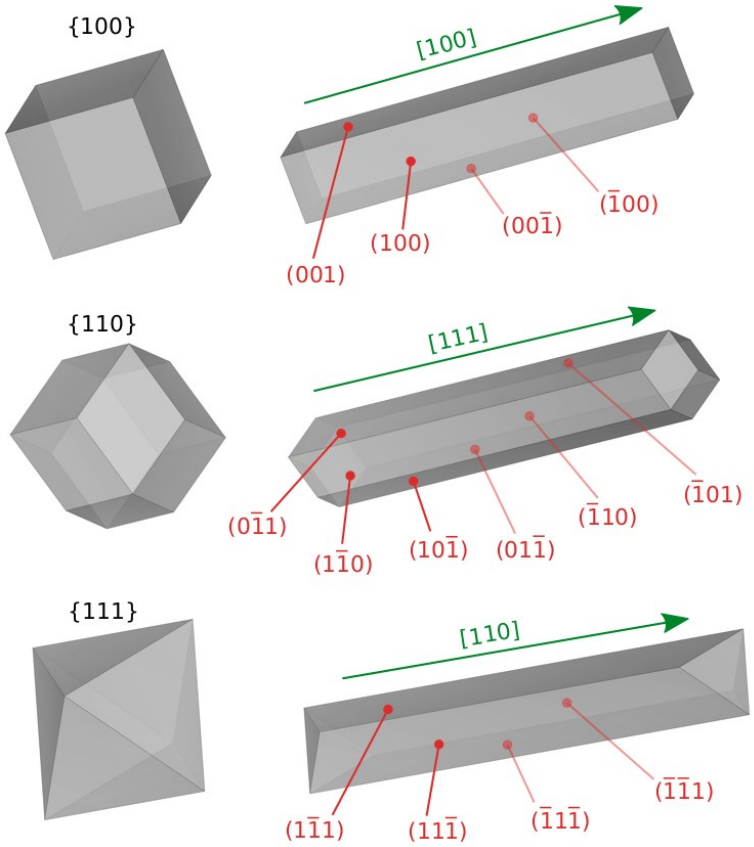

Figure S1: *Simulation of whisker growth due to a symmetry breaking for {100}, {110}, and {111}-dominated Wulff shapes. The (hkl)-surfaces which are favored (lower surface tension and higher surface area) and the [hkl]-growth directions are highlighted in red and green, respectively.*

B. Energy lowering induced by symmetry breaking

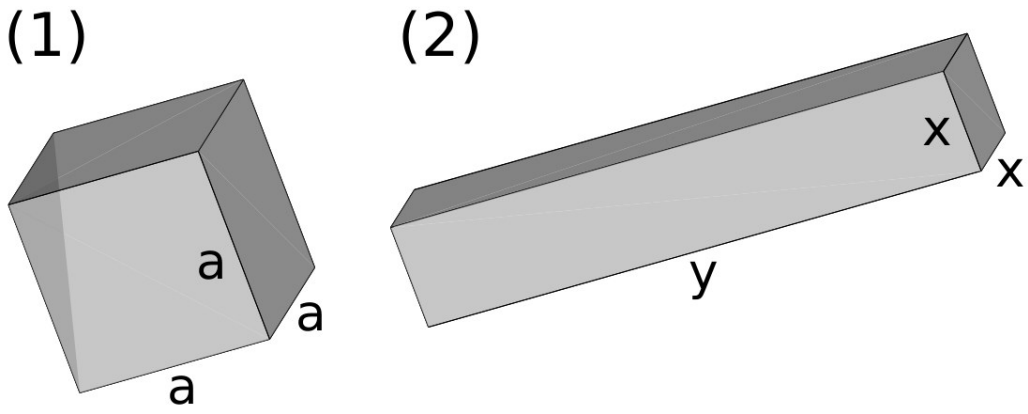

For the initial system (1) which is a cube, the volume $V^{(1)}$ and the total energy $E^{(1)}$ are introduced as:

$V^{(1)} = a^3$ $E^{(1)} = E_{bulk} + E_{surf}6a^2$

where E_{bulk} and E_{surf} are the bulk energy and the surface energy, respectively. For the final system (2) which is a whisker:

$V^{(2)} = x^2y$ $E^{(2)} = E_{bulk} + E_{surf}(2x^2 + 4xy)$

If we consider the condition that the volume is kept constant:

$a^3 = x^2y$ $x = a^{3/2}/y^{1/2}$

Then the energy difference between the two systems is:

$\Delta E = E^{(2)} - E^{(1)}$

$\Delta E = E_{surf}(2x^2 + 4xy - 6a^2)$

$\Delta E = E_{surf}(2a^3y^{-1} + 4a^{3/2}y^{1/2} - 6a^2)$

We consider that $y >> a$, therefore leading to the conclusion that ΔE has the same sign that E_{surf}. Thus:

- When $E_{surf} > 0$: $\Delta E > 0$: the cube is favored over the whisker for positive surface energy.
- When $E_{surf} < 0$: $\Delta E < 0$: the whisker is favored over the cube for negative surface energy.

S3. Potential of zero-charge

The potential of zero-charge E_M^{PZC} of a metal particle *M* corresponds to the potential value for which the surface charge of the particle is equal to zero. E_M^{PZC} is determined by calculating the surface charge of the global particle Qs (composed by different (hkl) surfaces) to different potential values. For each potential value, the surface charge of the particle is determined as follows: first, the Wulff shape is built to obtain the area fraction A_{hkl} of each (hkl)-surfaces present on the particle structure. Then the surface charge of the particle is computed as the sum of the charges q_{hkl} of each (hkl)-surfaces pondered by their respective area fraction:

$$Q_s = \sum_{hkl} q_{hkl} A_{hkl}$$

E_{Li}^{PZC} computed in PCM@Li (Fig.S2) and PCM@Li-CO_3 are equal to +1.53V/Li and +1.56V/Li, respectively. E_{Na}^{PZC} and E_{Mg}^{PZC} computed in PCM conditions are equal to +0.94V/Na and +1.58V/Mg, respectively.

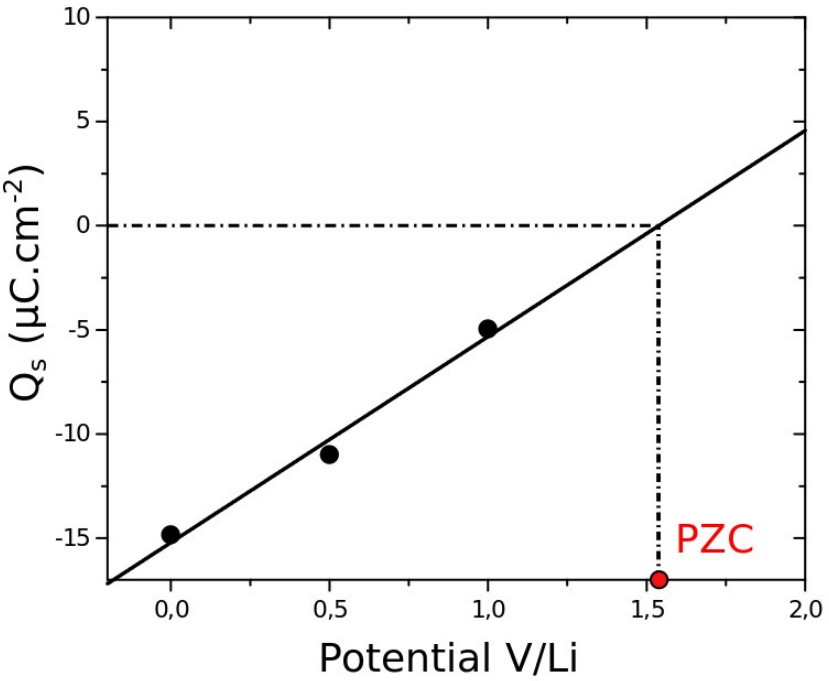

Figure S2: *Graphical representation of the potential-dependent surface charge of the lithium particle computed in PCM@Li conditions. The lithium particle surface charge is computed as the sum of each* (hkl)*-surface charges pondered by their area fractions, as indicated on Wulff shape.* E_{Li}^{PZC} *corresponds to the potential value for which the lithium particle is globally uncharged (Qs = 0), and is equal to +1.53V/Li.*

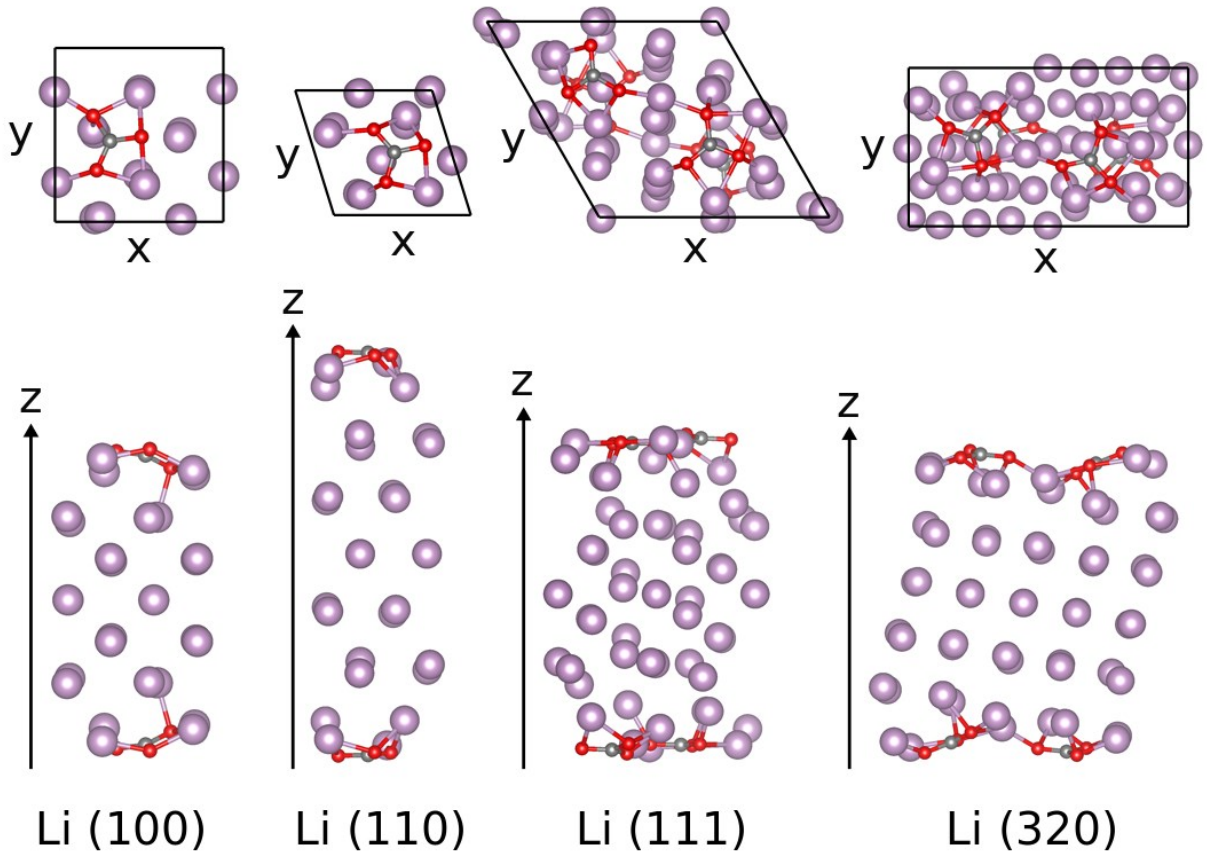

Figure S3: *Li/carbonate unit cells after relaxation, used for PCM@Li-CO_3 DFT calculations: top and side views for Li(100), Li(110), Li(111) and Li(320) from left to right. Cells are symmetric, the thickness of the vacuum region is fixed to 25Å, and the thickness of the metallic region is 10.32Å, 14.60Å, 11.92Å and 12.40Å for Li(100), Li(110), Li(111) and Li(320), respectively. The size of the supercells and the number of carbonate(s) added on the surfaces were chosen in order to maintain a carbonate surface density approximately constant (~ 1 carbonate for 50$Å^2$ = 0.020 carbonate.$Å^{-2}$). Carbonate surface density is 0.021 carbonate.$Å^{-2}$, 0.020 carbonate.$Å^{-2}$, 0.021 carbonate.$Å^{-2}$ and 0.023 carbonate.$Å^{-2}$, respectively for Li(100), Li(110), Li(111) and Li(320).*

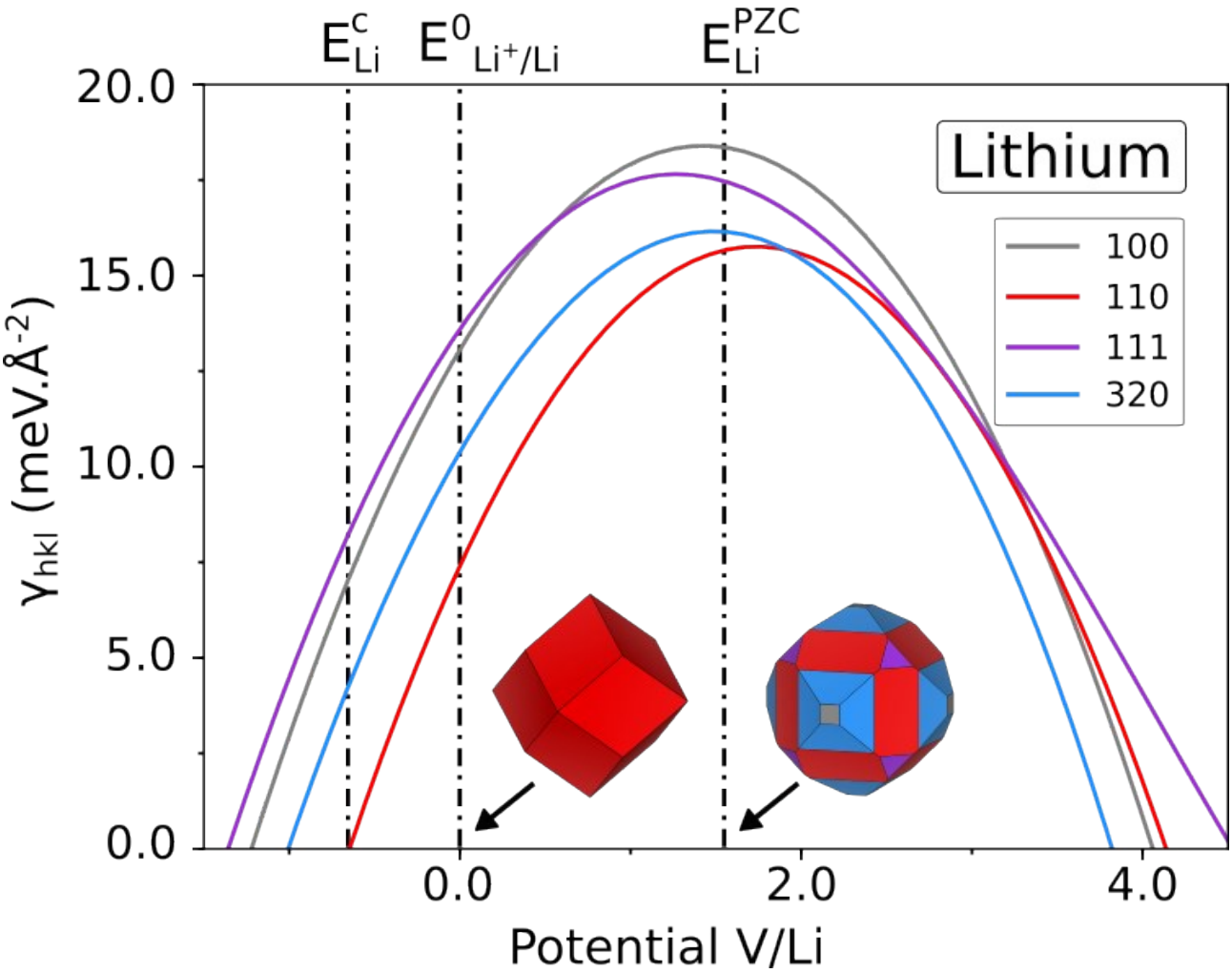

Figure S4: *Lithium electro-capillary diagram as computed within the grand canonical DFT approach in PCM@Li-CO_3 conditions.* E^{PZC}_{Li} *= +1.56V/Li corresponds to the potential computed for the zero-charged Li-particles. The critical potential* E^{c}_{Li} *allows to determine the lithium critical over-potential defined as* $\Delta E^{c}_{Li} = E_{Li^+/Li}^{0} - E^{c}_{Li}$ *= +0.65V/Li. The evolution of Li-particles shape, as obtained from a potential-dependent Wulff approach, is shown for various electrode potentials at* E *= 0 V/Li and +1.56 V/Li (oxidative conditions).*

S4. Parametrization for the PCM@Li-CO_3 calculations

For PCM@Li-CO_3 calculations, a PCM parametrization different from the one used in PCM@Li calculations was required to avoid unphysical electron solvation between the adsorbed species and the implicit solvent. As a consequence, surface capacitances of carbonated interfaces (PCM@Li-CO_3) were artificially decreased compared to carbonate-free interfaces (PCM@Li) and experimental ones, which has no physical meaning. Indeed, chemical adsorption of carbonate species on the surface of a Li-metal electrode is expected to affect the surface dipole and favors charge-excess delocalization, which in turns decreases the surface tension and increases the surface capacitance. To allow reliable comparison between PCM@Li and PCM@Li-CO_3 interface calculations, the surface capacitances obtained in explicit conditions were extrapolated to the one obtained in implicit conditions that were already shown to be in fair agreement with experimental data (vide supra). At first sight arbitrary, this scaling factor is physically relevant as it sets the lower-bound of the effect of explicit solvation on surface capacitances.

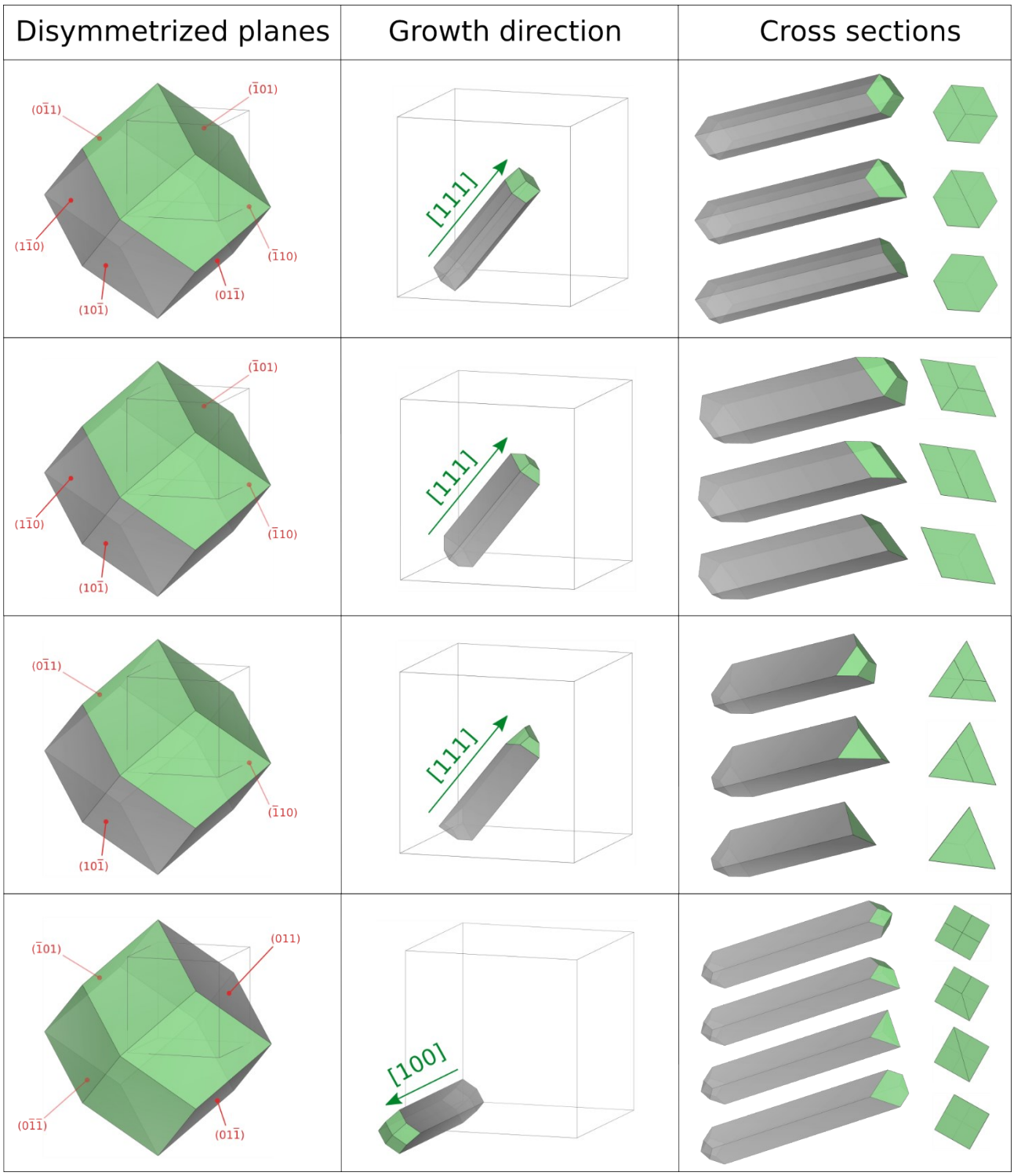

Figure S5: *Symmetry lowering for a {110}-faceted particle. The [111] growth-direction can lead to hexagonal, rhombus or triangular cross sections while the [100] growth-direction leads to square cross sections.*

(hkl)-surface	E_{hkl}^{PZC} *(V/Li)*	Υ_{hkl}^{PZC} *(meV.Å^{-2})*	C_{hkl}^{s} *(µF.cm^{-2})*
(100)	*1,53*	*29,08*	*7,50*
(110)	*1,67*	*30,68*	*8,46*
(111)	*1,24*	*32,82*	*7,46*
(210)	*1,47*	*30,84*	*7,66*
(211)	*1,53*	*33,37*	*7,62*
(221)	*1,25*	*32,44*	*7,72*
(310)	*1,50*	*31,12*	*7,34*
(311)	*1,43*	*32,43*	*6,73*
(320)	*1,49*	*30,80*	*7,14*
(321)	*1,47*	*33,03*	*7,91*
(322)	*1,35*	*33,47*	*6,79*
(331)	*1,26*	*32,45*	*7,14*
(332)	*1,26*	*32,82*	*7,40*

Table S1: *Calculated values for lithium (hkl)-surfaces in PCM conditions.*

(hkl)-surface	E_{hkl}^{PZC} *(V/Li)*	Υ_{hkl}^{PZC} *(meV.Å-2)*	C_{hkl}^{s} *(µF.cm-2)*
(100)	*1,42*	*18,40*	*8,39*
(110)	*1,74*	*15,76*	*8,91*
(111)	*1,23*	*17,61*	*8,43*
(320)	*1,50*	*16,17*	*8,20*

Table S2: *Calculated values for lithium (hkl)-surfaces in PCM@Li-CO_3 conditions.*

(hkl)-surface	E_{hkl}^{PZC} *(V/Na)*	Υ_{hkl}^{PZC} *(meV.Å^{-2})*	C_{hkl}^{s} *(µF.cm^{-2})*
(100)	*0,87*	*13,74*	*7,56*
(110)	*1,03*	*13,19*	*7,46*
(111)	*0,78*	*15,61*	*7,79*
(210)	*0,91*	*14,07*	*7,24*
(211)	*0,91*	*14,85*	*7,37*
(221)	*0,88*	*15,05*	*7,27*
(310)	*0,88*	*14,28*	*7,53*
(311)	*0,86*	*14,83*	*7,21*
(320)	*0,95*	*13,81*	*7,02*
(321)	*0,93*	*14,40*	*7,53*
(322)	*0,86*	*15,24*	*7,18*
(331)	*0,91*	*14,62*	*7,02*
(332)	*0,83*	*15,22*	*7,53*

Table S3: *Calculated values for sodium (hkl)-surfaces in PCM conditions.*

(hkil)-surface	E_{hkl}^{PZC} *(V/Mg)*	Υ_{hkl}^{PZC} *(meV.Å^{-2})*	C_{hkl}^{s} *(µF.cm^{-2})*
(0001)	*1,55*	*33,97*	*7,91*
$(10\bar{1}0)$	*1,48*	*40,21*	*7,53*
$(10\bar{1}1)$	*1,55*	*41,06*	*7,27*
$(10\bar{1}2)$	*1,51*	*45,12*	*7,59*
$(11\bar{2}0)$	*1,34*	*47,26*	*7,98*
$(21\bar{3}0)$	*1,34*	*45,88*	*7,62*

Table S4: *Calculated values for magnesium (hkil)-surfaces in PCM conditions.*

Metal (M)	*(hkl)-surface*	$E_{CO_3^{2-}}^{ads}$ *(eV)*	ΔE_M^c*(V/M) PCM*	ΔE_M^c*(V/M) PCM@CO_3*
Li	*(110)*	*0*	*+1.71*	*+0.65*
Na	*(110)*	*0.268*	*+1.37*	*+0.59*
Mg	*(0001)*	*0.007*	*+2.42*	*+1.42*

Table S5: *Adsorption energies (referenced to the adsorption energy of carbonate on Li surface) and critical overpotentials, as computed for Li, Na and Mg surfaces in PCM and PCM@CO_3 conditions. The (hkl)-surfaces considered are the first reaching the critical overpotential value. Note that ΔE_M^c in PCM@CO_3 for Li comes from its electro-capillary curve computed within the explicit approach (Fig. S4), while Na and Mg ones are extrapolated from purely implicit surface tension, shifted by the carbonate surface adsorption energy for Na and Mg respectively (vide supra).*

1. Filhol, J.-S. & Neurock, M. Elucidation of the Electrochemical Activation of Water over Pd by First Principles. *Angew. Chem. Int. Ed.* **45**, 402–406 (2006).
2. Mamatkulov, M. & Filhol, J.-S. An abinitio study of electrochemical vs. electromechanical properties: the case of CO adsorbed on a Pt(111) surface. *Phys. Chem. Chem. Phys.* **13**, 7675 (2011).
3. Kopač Lautar, A., Hagopian, A. & Filhol, J.-S. Modeling interfacial electrochemistry: concepts and tools. *Phys. Chem. Chem. Phys.* **22**, 10569–10580 (2020).
4. Momma, K. & Izumi, F. *VESTA 3* for three-dimensional visualization of crystal, volumetric and morphology data. *J. Appl. Crystallogr.* **44**, 1272–1276 (2011).